

# Thermodynamic properties of snow cover on sea ice during the austral summer in Prydz Bay, East Antarctica

HAN Hongwei<sup>\*</sup>, CHENG Peng<sup>1</sup>, LI Zhijun<sup>1</sup>, LEI Ruibo<sup>2</sup> & LU Peng<sup>1</sup>

<sup>1</sup> State Key Laboratory of Coastal and Offshore Engineering, Dalian University of Technology, Dalian 116024, China;

<sup>2</sup> Polar Research Institute of China, Shanghai 200136, China

Received 30 July 2013; accepted 13 February 2014

**Abstract** The thermodynamic properties of snow cover on sea ice play a key role in the ice-ocean-atmosphere system and have been a focus of recent scientific research. In this study, we investigated the thermodynamic properties of snow cover on sea ice in the Nella Fjord, Prydz Bay, East Antarctica (69°20'S, 76°07'E), near the Chinese Antarctic Zhongshan Station. Our observations were carried out during the 29th Chinese National Antarctic Research Expedition. We found that the vertical temperature profile of snow cover changed considerably in response to changes in air temperature and solar radiation during the summer. Associated with the changes in the temperature profile were fluctuations in the temperature gradient within the upper 10 cm of the snow cover. Results of previous research have shown that the thermal conductivity of snow is strongly correlated with snow density. To calculate the thermal conductivity in this study, we measured densities in three snow pits. The calculated thermal conductivity ranged from 0.258–0.569 W·m<sup>-1</sup>·K<sup>-1</sup>. We present these datasets to show how involved parameters changed, and to contribute to a better understanding of melting processes in the snow cover on sea ice.

**Keywords** snow cover, temperature, density, summer, Antarctica

**Citation:** Han H W, Cheng P, Li Z J, et al. Thermodynamic properties of snow cover on sea ice during the austral summer in Prydz Bay, East Antarctica. *Adv Polar Sci*, 2014, 25: 10-16, doi: 10.13679/j.advps.2014.1.00010

## 1 Introduction

In the polar regions, sea ice cover provides a platform for the formation of snowpacks because the solid form is stable for a long time, whereas snow falling into ice-free water melts immediately. The thermodynamic properties of snow cover change as the snowpack hardens. The initial density of natural fresh snow is about 0.1 g·cm<sup>-3</sup>, while after 30 and 50 days at a relatively constant temperature of -13°C, the density increases to 0.3 and 0.4 g·cm<sup>-3</sup>, respectively<sup>[1]</sup>. In the past, researchers studying energy exchange over snow cover have had to use estimates of the thermal conductivity of snow based on regression equations relating to snow density. The thermal conductivity of snow is a function of snow density<sup>[2]</sup> and a value of 0.31 W·m<sup>-1</sup>·K<sup>-1</sup> has been used for the

thermal conductivity of snow in the majority of large-scale sea ice models<sup>[3-4]</sup>. There is a temperature differential with depth in the snow cover and the properties of snow are highly temperature-dependent<sup>[5]</sup>. Brandt and Warren<sup>[6]</sup> reported that temperature gradients in the snow affect ice-grain evolution and therefore the optical properties of the snowpack, and the optical properties in turn affect the vertical distribution of absorbed energy. Albert and McGilvary<sup>[7]</sup> suggested that the effects of heat transfer related to air flow in the snow are more obvious when there is a smaller temperature gradient over the entire snowpack and a higher rate of air flow in the snow than when there is a greater overall temperature gradient and a lower rate of air flow.

In the coastal regions of Antarctica winds are relatively strong as a result of the combined effects of katabatic and synoptic forcing<sup>[8]</sup>. Because persistently strong winds exist over the Antarctic sea ice, in particular immediately following

\* Corresponding author (email: hhw777@sina.com)

precipitation events<sup>[9]</sup>, wind-driven redistribution is a key factor influencing snow thickness<sup>[10]</sup>. Strong winds may remove snow from easily erodible surfaces and relocate it in accumulation areas, leading to substantial heterogeneity in snow cover<sup>[11]</sup>. The sculpting of the snow cover by wind causes anisotropy in the surface morphology of the underlying sea ice, augmenting the changes in thermodynamic characteristics (such as albedo and heat flux) in horizontal space. In general, the surface of the snow cover melts in summer because of warm temperatures and high solar radiation and the thermodynamic properties of the snow cover undergo rapid changes in the short term.

Here we present an analysis of observational data obtained during the 29th Chinese National Antarctic Research Expedition in Prydz Bay, East Antarctica. The purpose of this paper is to describe the thermodynamic properties of snow cover on sea ice during the austral summer. We perform multiple-parameter analysis, using data on temperature, vertical temperature gradient, temperature rise rate, and thermal conductivity in the snow cover. Melting takes place within the snow cover as thermal conditions change. At the same time, the density of the snow cover changes in summer, with a positive response to melt-water migration at all depths throughout the snow cover layer.

## 2 Materials and methods

### 2.1 Study area

Antarctic sea ice consists predominantly of young or first-year ice because most melts during the first summer after it forms<sup>[12]</sup>. Our observations were carried out during the 29th Chinese National Antarctic Research Expedition, and the study site was located near the Chinese Antarctic Zhongshan Station, in Prydz Bay, East Antarctica (69°20'S, 76°07'E). In most years the sea ice is first-year ice, but occasionally the ice does not melt completely in the summer and re-freezes, forming multi-year ice. Generally, the ice cover is present for no less than 10 months a year. The ice breaks up during January and February, and re-forms about 1 month later<sup>[13-15]</sup>. A large number of icebergs, including those calved from the Dalk Glacier, tend to ground offshore from the Larsemann Hills<sup>[16]</sup>. In this area the prevailing wind comes from the northeast, and this limits the clearing of winter ice and smaller icebergs from the shore<sup>[13,17]</sup>.

A 9-cm diameter ice core was drilled at the study site to determine crystal structure, and the result confirmed that the ice was first-year fast ice. There are many crushed icebergs in the study region, and the snow cover is unevenly distributed on the leeward side of these iceberg remnants. The distribution of snow cover on sea ice is influenced by a number of factors. There are obvious differences in the thickness and morphology of snow cover, and these differences are closely linked to features of the surface ice, including rifts, ridges, and icepacks<sup>[18-19]</sup>. Figure 1 shows the surface properties of sea ice. The surface appears rugged because of the snow cover and scattered ridges and the

snow cover follows a belt-shaped distribution, with the long axis consistent with the direction of the prevailing wind.

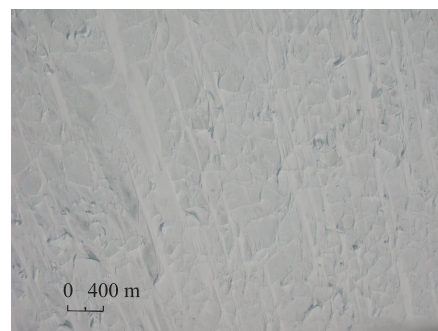


**Figure 1** Aerial photograph of the sea ice surface. Image captured on 1 December 2012 from an altitude of 210 m. The geographical position was 69°09'S, 76°07'E. The long axis of the belt-shaped snow cover distributed on the sea ice is consistent with the prevailing wind direction.

### 2.2 Observations

Figure 2 shows our study site among the belt-shaped snow cover on the leeward side of a crushed iceberg sculpted by the wind. The depth of the surrounding snow cover on the ice was about 5 cm in addition to the long belt-shaped snow cover. The maximum depth of the snow cover was about 90 cm, and the maximum width of the belt-shaped deposits was about 400 cm. We performed a total of four measurements during the period from 5–14 December 2012. Each sampling location was 100 cm from the previous one and the four sampling points were distributed along the long axis of the snow cover. At each sampling location we used a snow shovel to dig a snow pit vertical to the snow-ice interface. Because ice is harder than snow, it was easy to identify the snow-ice interface when digging the snow pits. We measured the snow depth from the surface of the snow cover to the snow-ice interface then measured the temperature of the snow cover. We used a wooden ruler to measure depths in the snow pits, and used a thermocouple thermometer probe embedded in the snowpack to measure temperature, recording until no significant fluctuation was observed to ensure the accuracy of the reading. The accuracy of the thermocouple thermometer probe was 0.1°C. Snow density was obtained by weighing a defined volume of the snow sample. We used a known volume cylinder sampling apparatus to collect the snow sample, and measured snow density using a volume method in a cold laboratory onboard the R/V *XUE LONG* icebreaker. For this study we used meteorological data recorded by the meteorological instruments onboard the R/V *XUE LONG* icebreaker.

## 3 Results and discussion

### 3.1 Meteorological conditions

Zhongshan Station has a climate typical of the Antarctic continent, specifically with low humidity, strong winds, and

low temperatures all year round with a large temperature difference between winter and summer<sup>[20]</sup>. A multi-year record of meteorological data was produced by averaging monthly values for 1989–2008, and the monthly mean temperature was between  $-4.4^{\circ}\text{C}$  and  $2.2^{\circ}\text{C}$  in the austral summer (December–February)<sup>[21]</sup>. The wind speed has an obvious annual variation at Zhongshan Station, tending to be higher in winter and lower in summer with gale-force winds rare in the summer months<sup>[20,22]</sup>.



**Figure 2** Photograph of the study site, located at  $69^{\circ}20'\text{S}$ ,  $76^{\circ}07'\text{E}$ .

The sky was mostly clear during the study period and there were no significant weather change events (Figure 3). From 1–2 December 2012, the air temperature decreased sharply from  $0.4^{\circ}\text{C}$  to  $-2.6^{\circ}\text{C}$  (Figure 3a) and the relative humidity increased and reached 77% on 2 December (Figure 3b). At the same time, wind speed peaked at  $7.9\text{ m}\cdot\text{s}^{-1}$ , the maximum value for the study period (Figure 3d). Relatively cold weather continued for 2 d, then, from 3–4 December, the air temperature increased from negative ( $-2.3^{\circ}\text{C}$ ) to positive ( $4.2^{\circ}\text{C}$ ), and the relative humidity decreased. In the following days (except 14 December) the air temperature stayed positive. There was no obvious change in atmospheric pressure from 5–9 December, but there was an increase from 9–13 December (Figure 3c).

### 3.2 Temperature, vertical temperature gradient, and temperature rise rate of snow cover

The surface of the snow was not completely smooth because of the effects of the wind; therefore the snow depth was different in each of our snow pits. The depths in the four snow pits were: 85 cm (5 December 2012),

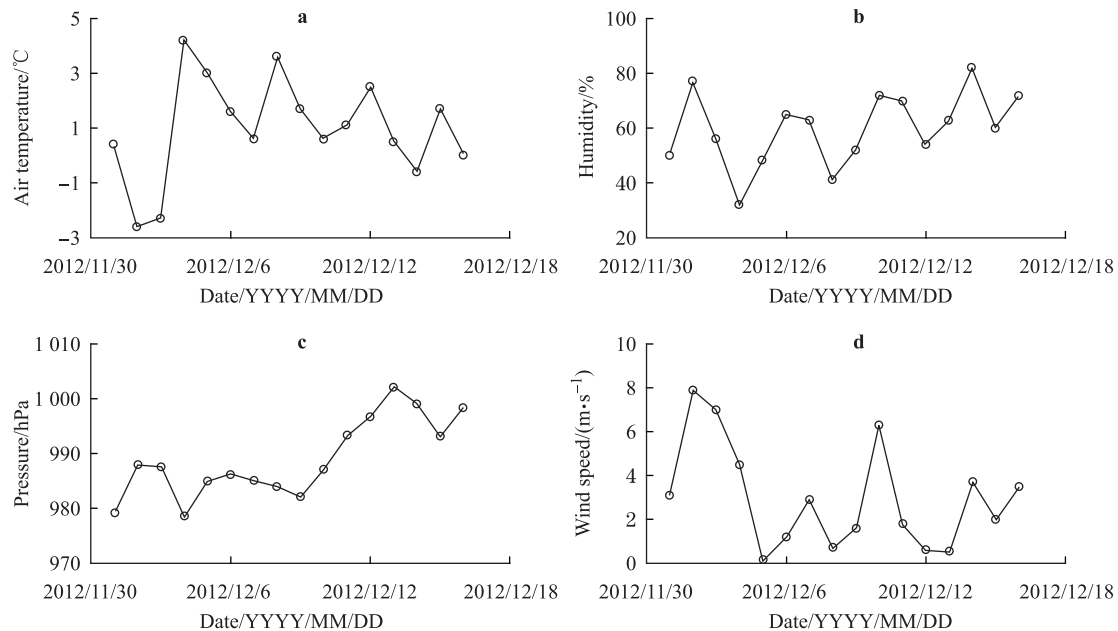


**Figure 3** Daily average temperature (a), humidity (b), pressure (c), and wind speed (d) throughout the study period.

85 cm (9 December), 90 cm (11 December), and 90 cm (14 December). Figure 4a shows the vertical temperature profiles of snow cover from the pit measurements (all the temperature profiles were recorded at about 15:00 local time). In the first pit dug in the snowpack on 5 December, the snow depth was 85 cm and the temperature was below  $-3^{\circ}\text{C}$  at depths from 17–85 cm. The lowest temperature was  $-3.9^{\circ}\text{C}$  at the snow-ice interface. From 0–35 cm in depth the temperature decreased gradually with an increase in depth, then did not change significantly below 35 cm. Comparison

between temperature data collected on 5 December and 9 December shows an increase in snow temperature. The most obvious change was that the  $-3^{\circ}\text{C}$  temperature layer migrated towards the lower stratum, to a depth of 55 cm. The third pit was dug on 11 December, with a depth of 90 cm. The data from this pit showed that the heating process was still evident in the snow cover. The inversion layer present at a depth of 70–90 cm may be a result of heat transport from migrated melt water (discussed in section 3.3). This inversion layer was not obvious in the fourth pit dug on 14

December. Data from this fourth pit showed that the surface temperature of the snow cover was lower than at the other three sites. The decrease in the surface temperature of the snow cover was the result of the lower air temperature on 14 December. The lowest temperature increased from  $-3.9^{\circ}\text{C}$  (5 December) to  $-2^{\circ}\text{C}$  (14 December) at the snow-ice interface. An increase in temperature will result in a decrease in the albedo of the snow and ice, and in turn an increase in solar energy absorption, which may result in melting of the snow and ice cover<sup>[23]</sup>. This positive feedback will accelerate the temperature change in the snow cover and lead to different vertical temperature profiles as recorded during the period from 5–14 December 2012.

For the purpose of this study, we presumed that the temperature differential only occurred in the vertical direction, not in the horizontal direction for the same depth layer. The temperature gradient is the ratio of the temperature differential to the distance between two isothermal surfaces in a specific direction (temperature gradient =  $-\nabla T/\nabla Z$ , where  $\nabla T$  is the temperature differential between two isothermal surfaces and  $\nabla Z$  is the distance between two isothermal surfaces in a specific direction). Figure 4b shows the temperature gradient at different depths of snow cover. The temperature gradient at the surface of the snow cover was not calculated because the air temperature field was not continuous with the snow cover. The temperature gradient showed an obvious fluctuation in the upper 10 cm of the snow cover, influenced by solar radiation and air temperature. At depths from 10 cm to the snow-ice interface, the temperature gradient ranged from  $-0.1^{\circ}\text{C}\cdot\text{cm}^{-1}$  to  $0.06^{\circ}\text{C}\cdot\text{cm}^{-1}$ .

Temperature rise rate is a parameter used to characterize the temperature change rate, and the unit is  $^{\circ}\text{C}\cdot\text{d}^{-1}$ . Solar heating is concentrated in the top few millimeters of the snow surface<sup>[6]</sup>. To eliminate the effect of surface temperature fluctuation caused by solar radiation on temperature rise rate, we studied the change of temperature rise rate at depths from 20 cm to the snow-ice interface. Figure 4c shows the temperature rise rate in different layers of the snow cover throughout the study period. From 5–9 December, the maximum temperature rise rate was  $0.53^{\circ}\text{C}\cdot\text{d}^{-1}$  at a depth of 20 cm. During this period, the temperature rise rate followed a linear decreasing trend with increasing depth. The temperature of the snow cover increased in the period 9–11 December (Figure 4a); however, the temperature rise rate followed different trends with increasing depth. From a depth of 20–30 cm, the temperature rise rate decreased compared with the previous period, but on the contrary, it increased at a depth of 30–80 cm depth. In the period from 11–14 December, from a depth of 20 cm to the upper boundary of the inversion layer (70 cm), the temperature rise rate showed a linear increasing trend with increasing depth. The results indicate that, during this last period, the temperature rise rate trend was in an opposite direction compared with the first period (5–9 December). This was because the increase in temperature had a lag effect with depth. As the temperature increased close to a temperature that would melt snow, the temperature rise rate decreased and

tended to become stable.

### 3.3 Density of snow

The time series of density measurements obtained from the snow cover is shown in Figure 5. Density measurement was carried out on 5 December, 9 December, and 11 December 2012. The results show that the density was greater than  $0.4\text{ g}\cdot\text{cm}^{-3}$  throughout the snow cover layer in summer. This value is significantly higher than the density of fresh snow<sup>[24–25]</sup>. Allworth<sup>[26]</sup> suggested that snow cover densities could range from  $0.1\text{--}0.5\text{ g}\cdot\text{cm}^{-3}$ , depending on the wind conditions prior to deposition. On 5 December, the density measurement varied little between the different sampling layers. From the air-snow interface to a depth of 75 cm, the density was in the range of  $0.45\text{--}0.50\text{ g}\cdot\text{cm}^{-3}$ , and the density increased to  $0.55\text{ g}\cdot\text{cm}^{-3}$  in the lower 10 cm of the snow cover. This suggests that melting took place in the snow cover as the snow temperature increased. Comparison between the density data collected on 5 December and 9 December shows that the density increased significantly in the top few centimeters. When we collected snow samples in the bottom few centimeters on 9 December, water trickled from the snow samples. This is because the surface melting caused an increase in water content, and as the melt water migrated through the snow cover and collected in the bottom few centimeters, the snow at the bottom was turned into slush. This led to a density increment, and the density increased to  $0.79\text{ g}\cdot\text{cm}^{-3}$  in the lower 10 cm of the snow cover. As a result of moisture migration, there was a low-density area above the slush layer. The density change caused by the moisture migration was most clearly demonstrated in the third density measurement on 11 December. First, the density in the top few centimeters returned to the value recorded on 5 December, while from a depth of 10–30 cm the density was higher than the previous value. Second, the low-density area at the top of the slush layer had disappeared. Third, the melt water in the slush layer was squeezed into the sea ice, and the melting rate and water supply could not keep up with the rate of loss, so the density returned to  $0.5\text{ g}\cdot\text{cm}^{-3}$  in the bottom few centimeters. However, the density associated with the microstructural and mesostructural characteristics of the snow cover was not invariable in summer. The gravity-driven flow of melt water changed the density field of the snow cover; therefore, there was significant variation in density across the entire snow cover layer.

### 3.4 Thermal conductivity

Thermal conductivity ( $k_{\text{eff}}$ ) is an important thermodynamic property that governs heat transfer in snow<sup>[27]</sup>. It determines the rate of heat transfer at the earth's surface in snow-covered regions, and its vertical profile influences temperature gradients, which in turn drive the modification of the structure and physical properties of the snowpack, including the thermal conductivity itself<sup>[28]</sup>.

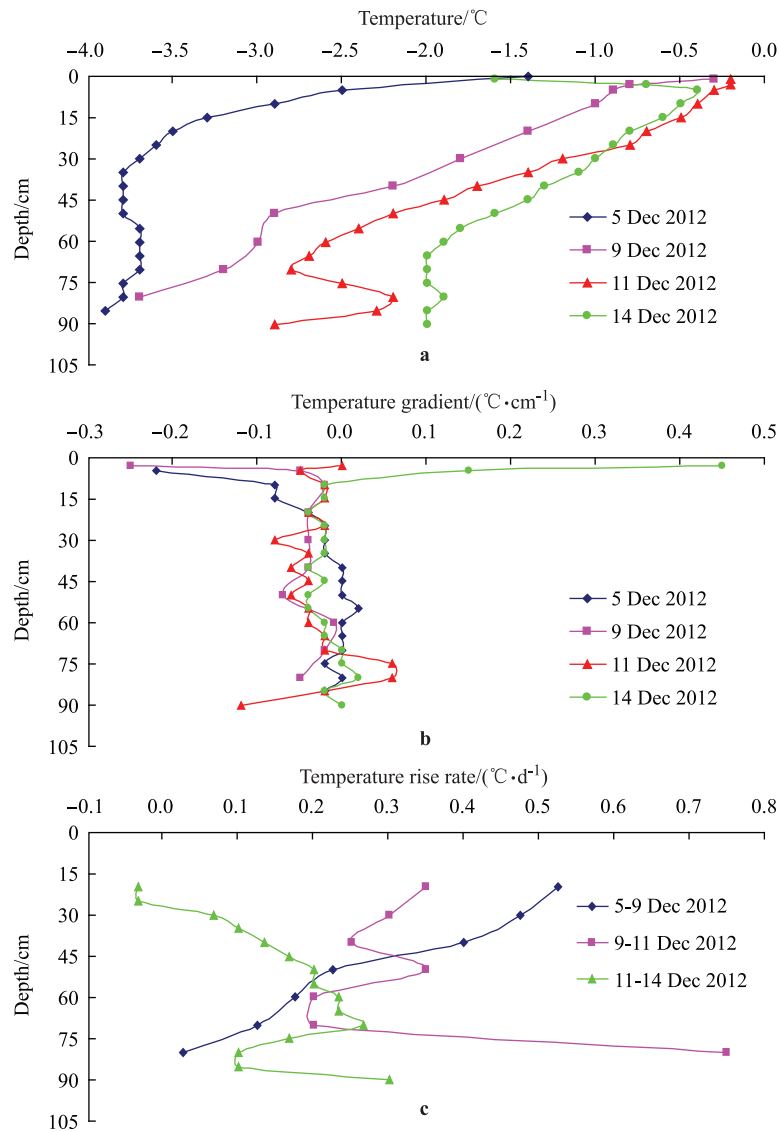


**Figure 4** The vertical profiles of temperature from pit measurements (a), temperature gradient (b), and temperature rise rate (c).

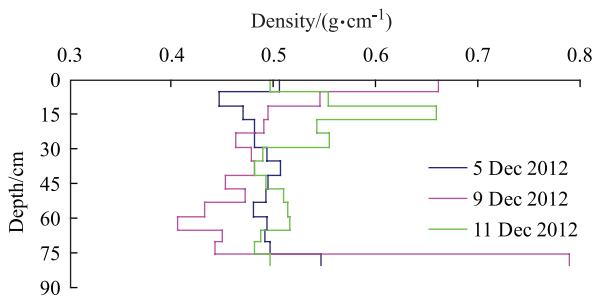


**Figure 5** Depth profiles of snow cover density.

The heated-needle probe technique has long been used for measuring the effective thermal conductivity of snow<sup>[29]</sup>. Some of the measurements in previous research were made in situ in the walls of snow pits, while others were made on snow samples that had been cut from the snow cover. Previous results show that thermal conductivity is strongly correlated

with snow density<sup>[27,30-31]</sup>. Empirical parameterizations that relate the thermal conductivity to the snow density have also been proposed<sup>[29,32]</sup>. Sturm et al.<sup>[29]</sup> proposed the following equations for seasonal snow:

$$k_{\text{eff}} = 0.138 - 1.01\rho + 3.233\rho^2 \quad 0.156 \text{ g}\cdot\text{cm}^{-3} \leq \rho \leq 0.6 \text{ g}\cdot\text{cm}^{-3} \quad (1)$$

$$k_{\text{eff}} = 0.023 + 0.234\rho \quad \rho < 0.156 \text{ g}\cdot\text{cm}^{-3} \quad (2)$$

The above equations were used to calculate the thermal conductivity from the densities measured in the three snow pits in the current study. As shown in Figure 6, the thermal conductivity varied from 0.258–0.569 W·m<sup>-1</sup>·K<sup>-1</sup>. We note that our results were consistent with results from previous studies. Reported correlations show  $k_{\text{eff}}$  values ranging from approximately 0.078 W·m<sup>-1</sup>·K<sup>-1</sup> for new snow to 0.290 W·m<sup>-1</sup>·K<sup>-1</sup> for a ubiquitous wind slab<sup>[30]</sup>. Morin et al.<sup>[28]</sup> found that the values of  $k_{\text{eff}}$  ranged between 0.004 W·m<sup>-1</sup>·K<sup>-1</sup> (freshly fallen snow) and 0.35 W·m<sup>-1</sup>·K<sup>-1</sup> (dense snow at the bottom of

the snowpack). It is also well known that snow structure and density affect thermal conductivity<sup>[29]</sup>. We can see that both wind slab and the dense snow at the bottom of the snowpack have higher thermal conductivity than the loose snow layer. The snow was transported by wind and accumulated, and there was no loose snow layer in the snow cover. The density of compact snow cover was greater than  $0.4 \text{ g}\cdot\text{cm}^{-3}$  across the entire layer in summer, so the calculated thermal conductivity was relatively high.

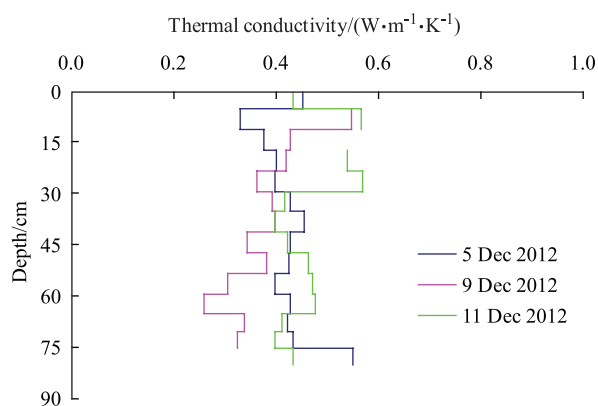


**Figure 6** Depth profiles of thermal conductivity. The thermal conductivity was not calculated when the density was greater than  $0.6 \text{ g}\cdot\text{cm}^{-3}$ .

## 4 Conclusions and future improvements

In December 2012, the thermodynamic properties of snow cover were measured during the 29th Chinese National Antarctic Research Expedition, in Prydz Bay, East Antarctica ( $69^{\circ}20'S$ ,  $76^{\circ}07'E$ ) near the Chinese Antarctic Zhongshan Station. We studied the snow cover on the leeward side of a crushed iceberg and the maximum depth was about 90 cm. During the study, the first field data (collected on 5 December) showed that the temperature was below  $-3^{\circ}\text{C}$  at depths from 17–85 cm, and the lowest temperature was  $-3.9^{\circ}\text{C}$  at the snow-ice interface. The temperature of the snow cover increased from the snow-ice interface to the surface, and the most significant observation was that the lowest temperature increased from  $-3.9^{\circ}\text{C}$  (on 5 December) to  $-2^{\circ}\text{C}$  (on 14 December) at the snow-ice interface. The temperature gradient was relatively stable throughout the study period. The temperature gradient fluctuated in the top few centimeters of the snow surface, and at a depth of 10 cm to the snow-ice interface, the temperature gradient was in the range of  $-0.1^{\circ}\text{C}\cdot\text{cm}^{-1}$  to  $0.06^{\circ}\text{C}\cdot\text{cm}^{-1}$ . The thermal conductivity of snow is a fundamental parameter in energy exchange and metamorphic processes within the snow cover. Previous research results have shown that the thermal conductivity is strongly correlated with snow density<sup>[25,27,30]</sup>. The density of snow cover was greater than  $0.40 \text{ g}\cdot\text{cm}^{-3}$  over the entire layer in summer, and in the range of  $0.40\text{--}0.79 \text{ g}\cdot\text{cm}^{-3}$ . The calculated thermal conductivity ranged from  $0.258\text{--}0.569 \text{ W}\cdot\text{m}^{-1}\cdot\text{K}^{-1}$ .

The thermodynamic properties of snow cover will

undergo a rapid change in summer, suggesting that snow cover physics will have to be incorporated into the atmosphere-ice-ocean system to properly represent snow surface mass and energy exchange. Snow plays two important but somewhat conflicting roles in the energy balance of the ice cover. On one hand, because of its high albedo, it reflects up to 85% of the incoming shortwave solar radiation<sup>[32]</sup>, significantly retarding melting in the spring<sup>[33]</sup>. On the other hand, because it is an excellent thermal insulator, snow decreases the rate of sensible heat transfer from the atmosphere. We will extend our future work to include the optical properties of snow cover, to better understand heat transfer mechanisms and the melting processes in the snow cover layer.

**Acknowledgments** This work is supported by the Foundation for Innovative Research Groups of the National Natural Science Foundation of China (Grant no. 51221961), the National Basic Research Program of China (Grant no. 2010 CB950301), and the International Science and Technology Cooperation Project (Grant no. 2011DFA22260). We also thank the crew of the R/V *XUE LONG* icebreaker for providing excellent logistic support. The 29th Chinese National Antarctic Research Expedition was organized by the Chinese Arctic and Antarctic Administration. The fieldwork was supported by the Polar Research Institute of China. Data were issued by the Data-sharing Platform of Polar Science (<http://www.chinare.org.cn>) maintained by Polar Research Institute of China (PRIC) and Chinese National Arctic & Antarctic Data Center (CN-NADC). The authors also wish to thank our colleagues who provided assistance during the ice camp.

## References

- 1 Yong R N, Metaxas I. Influence of age-hardening and strain-rate on confined compression and shear behaviour of snow. *J Terramech*, 1985, 22(1): 37-49.
- 2 Mellor M. Engineering properties of snow. *J Glaciology*, 1977, 19(81): 15-66.
- 3 Maykut G A, Untersteiner N. Some results from a time-dependent thermodynamic model of sea ice. *J Geophys Res*, 1971, 76(6): 1550-1575.
- 4 Semtner A J Jr. A model for the thermodynamic growth of sea ice in numerical investigations of climate. *J Phys Oceanogr*, 1976, 6(3): 379-389.
- 5 Reuter B, Schweizer J. The effect of surface warming on slab stiffness and the fracture behavior of snow. *Cold Reg Sci Technol*, 2012, 83-84: 30-36.
- 6 Brandt R E, Warren S G. Solar-heating rates and temperature profiles in Antarctic snow and ice. *J Glaciology*, 1993, 39(131): 99-110.
- 7 Albert M R, McGilvary W R. Thermal effects due to air flow and vapor transport in dry snow. *J Glaciology*, 1992, 38(129): 273-281.
- 8 Bintanja R. Characteristics of snowdrift over a bare ice surface in Antarctica. *J Geophys Res*, 2001, 106(D9): 9653-9659.
- 9 Massom R A, Lytle V I, Worby A P, et al. Winter snow cover variability on East Antarctic sea ice. *J Geophys Res*, 1998, 103(C11): 24837-24855.
- 10 Massom R A, Eicken H, Haas C, et al. Snow on Antarctic sea ice. *Rev Geophys*, 2001, 39(3): 413-445.
- 11 Déry S J, Yau M K. Large-scale mass balance effects of blowing snow and surface sublimation. *J Geophys Res*, 2002, 107(D23): 4679, doi: 10.1029/2001JD001251.
- 12 Allison I, Brandt R E, Warren S G. East Antarctic sea ice: Albedo,

- thickness distribution, and snow cover. *J Geophys Res*, 1993, 98(C7): 12417-12429.
- 13 Lei R B, Li Z J, Dou Y K, et al. Observations of the growth and decay processes of fast ice around Zhongshan Station in Antarctica. *Adv Water Sci*, 2010, 21(5): 708-712.
- 14 Lei R B, Li Z J, Cheng B, et al. Annual cycle of landfast sea ice in Prydz Bay, east Antarctica. *J Geophys Res*, 2010, 115(C2): doi: 10.1029/2008JC005223.
- 15 Lei R B, Li Z J, Zhang Z H, et al. Thermodynamic processes of lake ice and landfast ice around Zhongshan Station, Antarctica. *Adv Polar Sci*, 2011, 22(3): 143-152.
- 16 Yu Y, Li H R, Zeng Y X, et al. Bacterial diversity and bioprospecting for cold-active hydrolytic enzymes from culturable bacteria associated with sediment from Nella Fjord, Eastern Antarctica. *Mar Drugs*, 2011, 9(2): 184-195.
- 17 Tang S L, Qin D H, Ren J W, et al. Structure, salinity and isotopic composition of multi-year landfast sea ice in Nella Fjord, Antarctica. *Cold Reg Sci Technol*, 2007, 49(2): 170-177.
- 18 Palm S P, Yang Y K, Spinhirne J D, et al. Satellite remote sensing of blowing snow properties over Antarctica. *J Geophys Res*, 2011, 116(D16), doi: 10.1029/2011JD015828.
- 19 Déry S J, Tremblay L B. Modeling the effects of wind redistribution on the snow mass budget of polar sea ice. *J Phys Oceanogr*, 2004, 34(1): 258-271.
- 20 Yang Q H, Zhang L, Li C H, et al. Analysis on the variation tendencies of meteorological elements at Zhongshan Station, Antarctica. *Mar Sci Bull*, 2010, 29(6): 601-607.
- 21 Bian L E, Ma Y F, Lu C G, et al. Temperature variations at the Great wall Station (1985–2008) and Zhongshan Station (1989–2008), Antarctica. *Chinese J Polar Res*, 2010, 22(1): 1-9.
- 22 Xu C, Meng S, Li Y S, et al. The weather condition for aviation at Antarctic Zhongshan Station. *Martine Forecasts*, 2012, 29(1): 55-59.
- 23 Zhou X B, Li S S, Morris K, et al. Albedo of summer snow on sea ice, Ross Sea, Antarctica. *J Geophys Res*, 2007, 112(D16): doi: 10.1029/2006JD007907.
- 24 Judson A, Doesken N. Density of freshly fallen snow in the central Rocky Mountains. *Bull Amer Meteor Soc*, 2000, 81(7): 1577-1587.
- 25 Domine F, Albert M, Huthwelker T, et al. Snow physics as relevant to snow photochemistry. *Atmos Chem Phys*, 2008, 8(2): 171-208.
- 26 Aldworth E. Snow and ice characteristics of the Bellingshausen Sea, during the spring melt. *Deep-Sea Res II*, 1995, 42(4-5): 1021-1045.
- 27 Oldroyd H J, Higgins C W, Huwald H, et al. Thermal diffusivity of seasonal snow determined from temperature profiles. *Adv Water Res*, 2013, 55: 121-130.
- 28 Morin S, Domine F, Arnaud L, et al. In-situ monitoring of the time evolution of the effective thermal conductivity of snow. *Cold Reg Sci Technol*, 2010, 64(2): 73-80.
- 29 Sturm M, Holmgren J, König M, et al. The thermal conductivity of seasonal snow. *J Glaciology*, 1997, 43(143): 26-41.
- 30 Sturm M, Perovich D K, Holmgren J. Thermal conductivity and heat transfer through the snow on the ice of the Beaufort Sea. *J Geophys Res*, 2002, 107(C10), doi: 10.1029/2000JC000409.
- 31 Calonne N, Flin F, Morin S, et al. Numerical and experimental investigations of the effective thermal conductivity of snow. *Geophys Res Lett*, 2011, 38(23): L23501, doi: 10.1029/2011GL049234.
- 32 Barry R G. The parameterization of surface albedo for sea ice and its snow cover. *Prog Phys Geog*, 1996, 20(1): 63-79.
- 33 Sturm M, Holmgren J, Perovich D K. Winter snow cover on the sea ice of the Arctic Ocean at the Surface Heat Budget of the Arctic Ocean (SHEBA): Temporal evolution and spatial variability. *J Geophys Res*, 2002, 107(C10): 8047, doi: 10.1029/2000JC000400